Physiological
Measurement

PAPER • OPEN ACCESS

Heart-carotid pulse-wave velocity via laser-Doppler vibrometry as a biomarker for arterial stiffening: a feasibility study

To cite this article: Simeon Beeckman *et al* 2025 *Physiol. Meas.* **46** 045006

IOP Publishing Physiol. Meas. 46 (2025) 045006 https://doi.org/10.1088/1361-6579/adcb85

Physiological Measurement

IPEM Institute of Physics and Engineering in Medicine

OPEN ACCESS

RECEIVED
17 January 2025

REVISED
11 March 2025

ACCEPTED FOR PUBLICATION
10 April 2025

PUBLISHED
22 April 2025

PAPER

Heart-carotid pulse-wave velocity via laser-Doppler vibrometry as a biomarker for arterial stiffening: a feasibility study

Simeon Beeckman[1,*], Smriti Badhwar[2], Yanlu Li[3], Soren Aasmul[4], Nilesh Madhu[5], Hakim Khettab[6], Elie Mousseaux[6], Umit Gencer[2,6], Pierre Boutouyrie[2,6], Rosa Maria Bruno[2,6,7] and Patrick Segers[1,7]

[1] Simeon Beeckman and Patrick Segers are with IBiTech-BioMMedA, Ghent University, Ghent, Belgium
[2] Smriti Badhwar, Rosa Maria Bruno, Umit Gencer and Pierre Boutouyrie are with Paris Cardiovascular Research Center, INSERM U970, Paris, France
[3] Yanlu Li is with Photonics Research Group, Ghent University-IMEC, Technologiepark-Zwijnaarde 126, 9052 Ghent, Belgium
[4] Soren Aasmul is with Medtronic Bakken Research Center, Maastricht, The Netherlands
[5] Nilesh Madhu is with IDLab, Ghent University—imec, Ghent, Belgium
[6] Hakim Khettab, Elie Mousseaux, Umit Gencer, Pierre Boutouyrie and Rosa Maria Bruno are with Assistance Publique—Hôpitaux de Paris, Paris, France
[7] Both authors contributed equally.
[*] Author to whom any correspondence should be addressed.

E-mail: simeon.beeckman@ugent.be

Keywords: laser Doppler vibrometry, biosignal processing, arterial stiffness, heart-carotid pulse transit time, Sphygmocor, InSiDe Horizon 2020

Abstract

Objective. Large artery stiffening leads to an increase in cardiovascular risk and organ damage of the kidneys, brain or the heart. Biomarkers that allow for early detection of this phenomenon are a point of interest in research, with pulse-wave velocity (PWV) having been proven useful in predicting and monitoring arterial stiffness. We previously introduced a laser Doppler vibrometry (LDV) prototype which can measure carotid–femoral PWV (cfPWV). In this work, we assess the feasibility of using the same device to infer heart-carotid pulse-transit time (hcPTT) as a first step towards measuring heart-carotid PWV (hcPWV). The advantage of hcPWV over cfPWV is that the ascending aorta, which is the most distensible segment of the aorta contributing most to total arterial compliance, is included in the arterial pathway. *Approach*. Signals were simultaneously acquired from a location on the chest (near either the base or the apex of the heart) and the right carotid artery for 100 patients (45% female). Fiducial points on the heart waveforms are associated with opening and closure (second heart sound; S2) of the aortic valve, which can be combined with, respectively, the foot and dicrotic notch (DN) of the carotid waveform to retrieve hcPTT. Considering two distinct heart-signal measurement sites, four hcPTT estimations are evaluated in about 94% of all measurements. *Main results*. Correlations between these and known predictors of arterial stiffness i.e. age, blood pressure and carotid–femoral PTT via applanation tonometry indicated that combining S2 from a heart-measurement site located at the base of the heart, with the carotid DN yields hcPTT providing convincing correlations with known determinants of arterial stiffness ($\rho = 0.377$ with age). *Significance.* We conclude that LDV may provide a corollary biomarker of arterial stiffness, encompassing the ascending aorta.

1. Introduction

The large arteries, and specifically the aorta, play a central role in the blood circulation (Wolinsky and Glagov 1967). Their structure allows the vessel wall to distend during cardiac contraction, storing elastic energy, which is used during the consequent relaxation to drive blood flow after the pressure wave has passed (Wolinsky and Glagov 1967, Parker 2009, Westerhof *et al* 2009). This way, a near-continuous flow is assured further down the arterial tract, providing constant organ perfusion. This buffer or 'windkessel' function deteriorates significantly when large arteries stiffen, during a process called arteriosclerosis, leading to

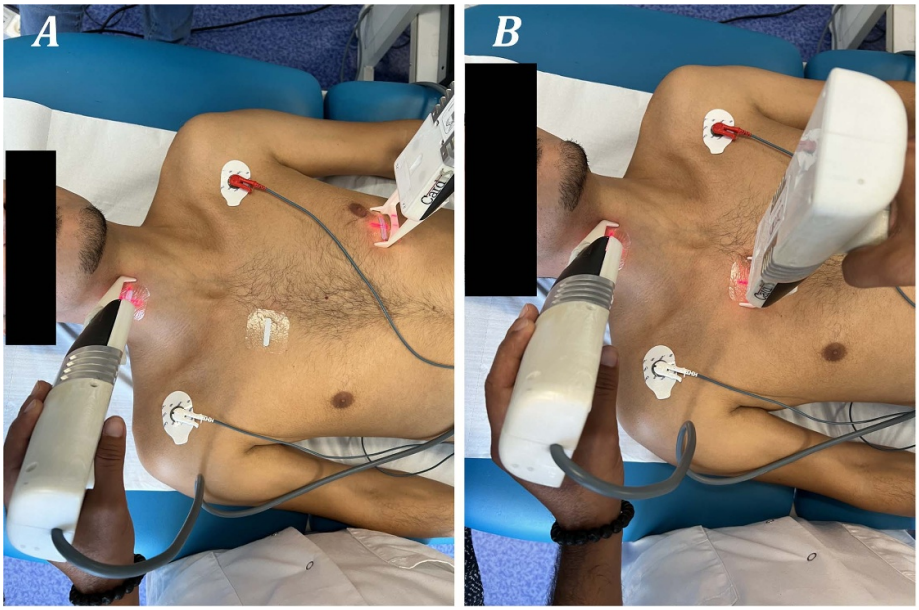

Figure 1. Overview of the two investigated methodologies to achieve hcPTT. Both panels show the LDV device's two handpieces measuring in parallel. The left panel shows a measurement on the carotid artery and the fifth left intercostal space. The right panel presents a measurement on the carotid artery and second right intercostal space.

deregulated blood pressure, blood flow and consequent organ damage (Laurent *et al* 2006, Vlachopoulos *et al* 2010, Ben-Shlomo 2014, Chirinos *et al* 2019). Understanding the associated waveforms in blood pressure and flow related signals is vital in detecting and preventing this early vascular aging (Alastruey 2023).

1.1. Carotid–femoral pulse-wave velocity (cfPWV)

A metric that allows for quantifying arterial stiffening is PWV (Laurent *et al* 2006, Boutouyrie and Bruno 2019, Segers *et al* 2020), with especially cfPWV being studied and showing a significant relationship with arterial stiffness. It can be stated that cfPWV serves as the baseline biomarker regarding arterial stiffening (Segers *et al* 2020). The speed of the pulse-wave induced by heart-contraction increases with increased arterial stiffness. If one measures the arrival time of the pulse-wave at two distinct points on the arterial tract, separated by a distance dx, one can calculate PWV as in equation (1), where PTT is the delay in the pulse arrival time (PAT) across the two points. We refer to PTT as the pulse-transit time (PTT),

$$\mathrm{PWV} = \frac{dx}{\mathrm{PTT}}. \tag{1}$$

Aside from the current state-of-the-art measurement methods of cfPWV, such as applanation tonometry and ultrasound (US) (Pereira *et al* 2015, Segers *et al* 2020), we have been exploring an alternative approach based on laser-Doppler vibrometry (LDV) (De Melis *et al* 2008, Campo and Dirckx 2011, Kaplan *et al* 2012). With this technique, skin displacement signals above large arteries such as the carotid and femoral arteries can be measured, from which the PAT and carotid–femoral PTT (cfPTT) can be estimated (Li *et al* 2013). It was shown that cfPWV via LDV measurements had a high agreement with its tonometry-based counterpart (Badhwar 2024)

1.2. Heart-carotid PWV (hcPWV)

A drawback of cfPWV is that its arterial pathway does not include the ascending aorta, which is the most distensible aortic segment and consequently the region where the increase in arterial stiffness is expected to be most apparent. cfPWV is determined using a pathway spanning from the femoral artery up to the descending thoracic aorta. In this way, an important region of potential elastic behavior changes is excluded from the metrics. Vlachopoulos *et al* have shown that aortic stiffness is an independent predictor of cardiovascular-related mortality and disease (2010), that also precedes the onset of hypertension (Mitchell *et al* 2010).

This work proposes heart-carotid PTT (hcPTT) as an additional biomarker that includes the ascending aorta. Our hcPTT is measured via LDV, as seen in figure 1, as opposed to the more frequent use of MRI to assess aortic stiffness (Yong Kim 2007, Ou *et al* 2008a, 2008b, Redheuil *et al* 2010, van Elderen *et al* 2010, Dogui *et al* 2011, Brandts *et al* 2012, Bensalah *et al* 2014). A similar experiment was conducted previously,

using accelerometers placed on the chest at the mid-sternal precordial region, and in the neck above the carotid artery (Faita *et al* 2009). This experiment was able to evaluate the variation of the true central hcPTT during pharmacological and dynamic stress. In general, hcPTT is calculated between the proximal measurement site (the heart), and the distal one of the carotid (Mukkamala *et al* 2015).

Approaches for the proximal measurement site have been proposed, among them seismocardiography (SCG) (Di Lascio *et al* 2014, Crow *et al* 2017, Yang and Tavassolian 2018, Balali *et al* 2022). SCG also measures skin acceleration, albeit via different technology and methodology, and could thus be interpreted as a form of reference for the currently unexplored LDV heart-waveforms. Phonocardiogram (PCG) methods via digital stethoscope have also been investigated for the proximal measurement (Park *et al* 2022). Regarding the distal waveform, LDV can provide reliable waveforms at the carotid (Li *et al* 2013, Li 2020, Mancini *et al* 2020).

The specific research aims for this article are fourfold: assessing (i) correlation of hcPTT with relevant clinical parameters such as age and blood pressure; (ii) agreement of LDV with the golden standard for cfPTT, as measured by the Sphygmocor system; (iii) agreement between different estimates of hcPTT using LDV; (iv) investigation of the reproducibility of the LDV measurements. From these avenues, we propose an approach for the assessment of hcPTT while simultaneously quantifying the potential usefulness of hcPTT as a biomarker.

2. Materials & methods

2.1. The LDV-prototype specifications

In the context of a H2020 project (CARDIS, Grant agreement ID: 644 798), a first LDV prototype was constructed, which has been extensively described in Mancini *et al* (2019, 2020), Li (2020). Briefly, the device includes two handpieces, with which skin displacement can be simultaneously measured at two different locations. Each handpiece captures data using six laser beams with a wavelength of 1550 nm that are reflecting off of a retroreflective tape that is applied to the measurement site. The inter-beam distance is 5 mm. The displacement signals obtained are differentiated twice, yielding skin acceleration. The time-point of the arrival of the pulse wave is then detected by selecting the appropriate features in the acceleration signals.

2.2. Study population and data collection

In this study, 100 patients with ages ranging from 18 to 90 years old, that could provide informed, written consent were recruited after their routine clinical care. Population statistics are listed in table 1. Exclusion criteria for the InSiDe study were:

- Patients with skin lesions on the chest or neck or allergies to the adhesive that may affect placement of the patch.
- Patients with life-threatening conditions (metastatic cancer, end-stage renal failure, end-stage liver failure or end-stage heart failure).
- Patients with history of acute heart failure (NYHA class III–IV).
- Patients with progressive cardiovascular pathologies (unstable coronary artery disease, Peripheral artery disease, stroke, aortic dissection).
- Patients with arrhythmias leading to great heart rate variability during recordings.
- Pregnant or breastfeeding women.

The patients additionally underwent several tonometric and LDV measurements, with simultaneous recording of LDV signals at the two measuring sites as seen in figure 1. Patients were placed in a supine position for entire duration of the protocol. Tonometric cfPTT data was collected via the Sphygmocor system, to serve as an established biomarker to compare the LDV-results to. The following measurements were performed:

- cfPTT with the Sphygmocor system (three repeated measurements, measuring 10 heartbeats each).
- hcPTT, with the LDV probe measuring the heart signals aimed at the base of the heart (Base), as exemplified in panel (B) of figure 1(three repeated measurements, measuring 15 heartbeats each).
- hcPTT, with the LDV probe measuring the heart signals aimed at the apex of the heart (Apex). An example of this is shown in panel (A) of figure 1(three repeated measurements, measuring 15 heartbeats each).

Electrocardiogram (ECG) data were also collected in parallel with the LDV measurements. Brachial systolic and diastolic blood pressure (DBP) were gathered via state-of-the-art cuff-based technology.

Sphygmocor measurements were performed by continually recording ECG in parallel with the tonometry measurements. These alternate between measuring at the right carotid first, and then the right

Table 1. Population statistics. SD refers to standard deviation.

Parameter ($N = 100$)	Mean $\pm$ SD	Range
Age (years)	48 ± 17	[18, 81]
Sex (male %)	55	/
BMI (kg m^{-2})	26 ± 5	[17.24, 39.82]
Systolic BP (mmHg)	130 ± 20	[88, 219]
Diastolic BP (mmHg)	79 ± 15	[49, 136]

femoral artery. Transit time from the peak of the *R*-wave to the foot of the carotid pressure wave, and the peak of the *R*-wave to the foot of the femoral pressure wave, was used to calculate cfPTT. The intersecting tangent algorithm was used to assess the fiducial point of the foot of both pressure waveforms.

2.3. Analysis of heart-carotid LDV data

2.3.1. Data properties & preprocessing

For each measurement, six channels were measured for the carotid and heart measurement sites respectively. The signal length varied due to varying signal quality influencing the real-time heartbeat detection, but was capped at 60 s as a maximum measurement duration. All signals were passed through a second-order bandpass Butterworth filter with cutoff frequencies at 0.5 and 50 Hz respectively, to filter out baseline wandering and high-frequency signal distortion, and were then differentiated twice. The acceleration signals were then exported to the user at 10 kHz and were resampled to 1 kHz for post-processing computational purposes.

An example (patient 40, first Base-carotid measurement) is shown in figure 2. As can be observed in the figure, signal quality can vary drastically between channels and/or handpieces since it is possible that only a few beams are placed on top of the target artery (Seoni *et al* 2022). Panel (B) helps to visualize the arterial pathway between the measurement sites. The hcPTT to be quantified is the time delay between the pressure wave traveling from the aortic valve up to the right carotid artery, as demarcated in the figure panel.

A peak detection algorithm was applied to the ECG signal to detect the *R* waves of individual cardiac cycles. This allowed us to split the LDV signals into individual cardiac cycles, which will be called epochs in this work. Heart and carotid epochs that correspond to the same heartbeat are selected and matched to estimate the hcPTT based on the available temporal signal features. This is shown in figure 2, panel (C).

2.3.2. hcPTT calculation

Similar to carotid–femoral, we intended to identify signal features in the LDV traces that correspond to the same physical event in the cardiac cycle, for both the heart and the carotid epochs. For the interpretation of cardiac LDV skin-acceleration signals, we relied on what was reported on SGC data (Crow *et al* 2017, Balali *et al* 2022).

These SCG signals contain chest-skin acceleration in time, as measured by the application of accelerometers to the skin. From visual inspection of the data, it was found that the LDV signals mostly resembled the SCG waveforms as reported in literature. As indicated in panel (C) of figure 2, several signal features and their respective fiducial points could be indicated. For the heart-signal epoch, there is the mitral valve closure (MC), isovolumic contraction (IVC), aortic valve opening (AO), rapid ventricular ejection (RE), aortic valve closure (AC), mitral valve opening (MO) and rapid ventricular filling (RF). In the carotid signal-epoch we indicated the foot-of-the wave and dicrotic notch (DN), corresponding to AO and AC respectively. Two hcPTT estimation methods were proposed.

First, the features corresponding to the opening of the aortic valve were identified. For the carotid signals, this is the well-established foot-of-the-wave waveform (Segers *et al* 2020). Opening of the aortic valve is less evident to assess from the cardiac LDV data. Analyzing reported SCG data, the second peak in the first region of elevated signal energy after the timepoint of the ECG *R*-peak is associated with AO (Crow *et al* 2017, Balali *et al* 2022). It was assumed that, because of the similarity between SCG and chest-LDV waveforms, the same peak in the LDV signal also corresponded to AO. The time delay between these carotid and heart features was then taken as a first hcPTT estimation (PTT_1).

Secondly, the features corresponding to the closure of the aortic valve are considered, see panel (C) of figure 2. Again, this was straightforward to assess from the carotid data, where the well-known DN (Segers *et al* 2020) leads to a prominent second peak in the LDV acceleration signal. As for the heart signal, we again rely on what is known from SGC, where the first peak in the second region of visible signal perturbation (which we refer to as heartsound two, or S2) is associated with AC (Crow *et al* 2017, Balali *et al* 2022). Analogously, the corresponding LDV feature could be identified. Combining both features yielded a second

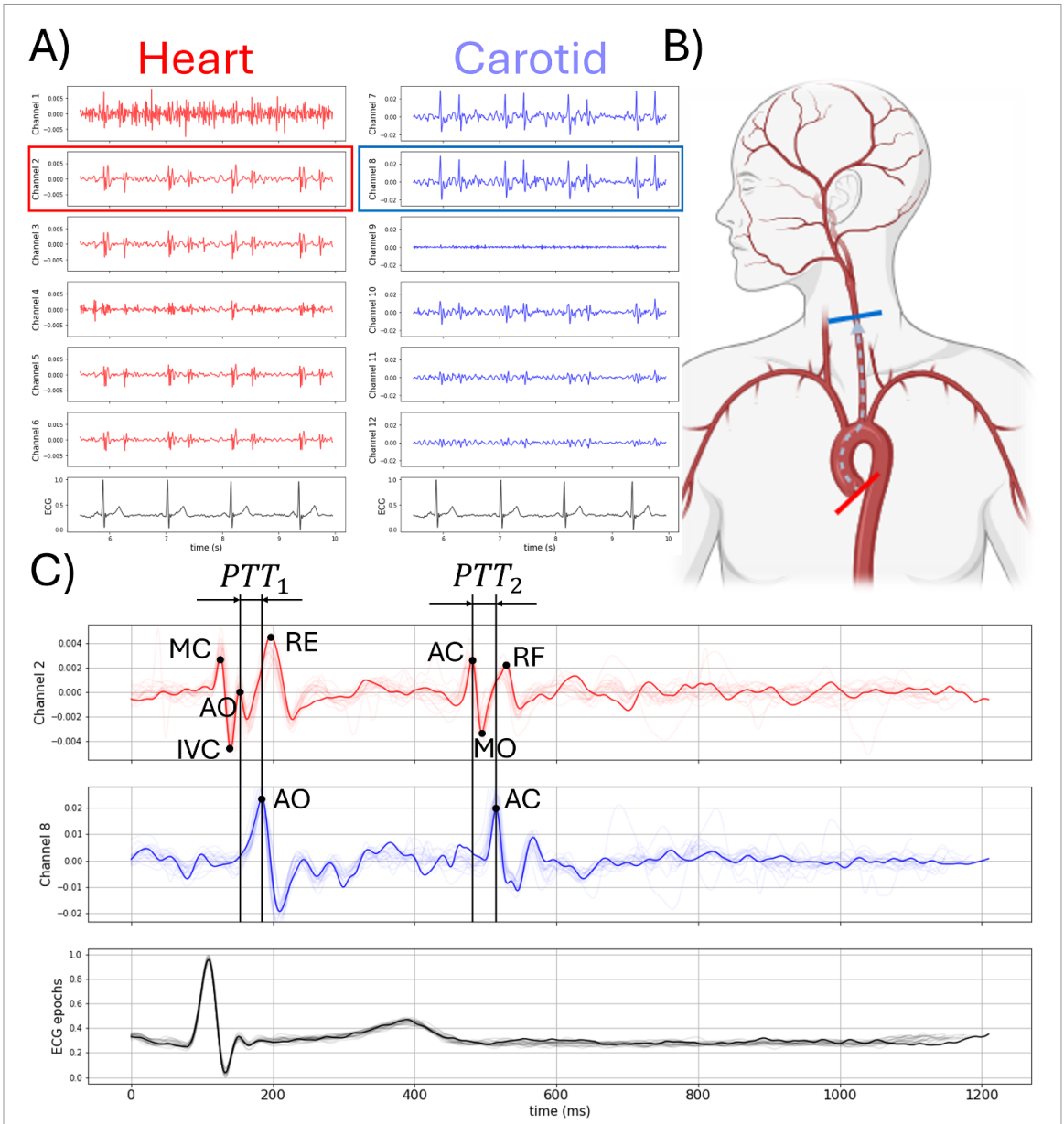

Figure 2. Panel (A) shows a 4.5 s segment of the first Base-carotid measurement of patient 40, performed during the study. The six channels in the right column represent carotid skin-acceleration in time. The left column contains base-of-the-heart skin acceleration in time. The bottom row shows the ECG measured in parallel with the LDV-channels. Panel (B) visualizes the arterial pathway under investigation. Figure created with BioRender.com. Panel (C) displays a selection of carotid (middle plot) and heart (upper plot) channels that were split into epochs using the ECG, shown in the bottom plot. A randomly-picked carotid and heart epoch are both displayed on top of all individual epochs. Two combinations of temporal features that lead to two distinct hcPTT estimations are illustrated. See text for the definition of all indicated points. *Y*-axes show arbitrary units for all graphs.

hcPTT estimation. In the following sections we will be referring to both these proposed methods as PTT_1 and PTT_2, respectively.

The following protocol was established to get PTT_1 and PTT_2, for Apex and Base measurements:

- For a given measurement (Base or Apex), the most qualitative channels (highest signal-to-noise ratio) of both handpieces respectively, were designated via visual inspection of signal quality.
- The *R*-wave peaks in the ECG trace were detected and utilized to split the selected channels into epochs.
- Signal averaging of the epochs yielded an average carotid and heart epoch.
- The five epochs per channel with the highest normalized cross-correlation coefficient with their average epoch were selected for hcPTT estimation.
- hcPTT estimation was performed via both methods described above to get PTT_1 and PTT_2 for the five selected epochs.
- Of these five values for both PTT_1 and PTT_2, the median values were taken as hcPTT estimates for the measurement.

- Of the three measurement hcPTT estimations per patient, the median value was again taken as final hcPTT estimation for the patient, and the standard deviation as a measure for inter-measurement hcPTT variability. If one (or two) of the three measurements could not be processed, the average value of the remaining hcPTT estimates was taken as the final hcPTT.

2.3.3. hcPTT with age and blood pressure

Both hcPTT estimation methods were applied on the database, for both heart-measurement sites. This resulted in four hcPTT estimations. All four were compared to known biomarkers for arterial stiffness: age, brachial DBP, brachial systolic blood pressure (SBP) and cfPTT measured via the Sphygmocor system. The same correlations were additionally calculated for both male and female patients separately. All correlations were quantified using the Pearson-correlation coefficient and were considered significant for associated p-values < 0.05. Variability between measurements done per patient was investigated.

Additionally, the agreement between the four methods was investigated. This was done through correlation analyses that were performed between hcPTT's estimated on the two different heart-measurement sites. Correlations between PTT_1 and PTT_2, controlling for measurement site, were also investigated as well as any statistical difference between the two metrics which was done via paired t-tests and nonparametric Wilcoxon signed-ranks tests. Bland–Altman plots were made to evaluate any potential biases and to appraise the level of agreement between hcPTT estimation methods and between heart-measurement sites.

2.3.4. Intra- and inter-operator variability

In order to examine the reproducibility of the hcPTT biomarker, a separate batch of measurements was performed on 10 healthy volunteers by two distinct operators (OP1 & OP2). Similar to the protocol of the InSiDe-study described above, every volunteer was subject to three LDV measurements at both Base and Apex, performed by the two operators. This resulted in a total of 120 planned measurements. It was determined that only subjects with all three measurements being processable, were considered for the reproducibility analysis. hcPTT's were derived from the considered measured data as mentioned before, and compared in an intra- and inter-operator analysis.

Intra-operator variability was quantified as follows: every measurement resulted in a hcPTT estimate. The coefficient of variation (CV) was calculated on the three hcPTT estimates per subject. For a single method, e.g. Base PTT_2, this resulted in 10 CV values of which the mean was taken, together with its standard error (SE), as the metrics for evaluation. This was done for Base PTT_1, Base PTT_2, Apex PTT_1 and Apex PTT_2. Equations (2) and (3) show the formulas used to calculate CV and SE σ refers to the standard deviation and μ to the arithmetic mean. σ_{CV} is the standard deviation of the CV values for the $N = 10$ subjects,

$$CV = 100 * \frac{\sigma}{\mu} \tag{2}$$

$$SE = \frac{\sigma_{CV}}{\sqrt{N}}. \tag{3}$$

The inter-operator variability was investigated using a Bland–Altman analysis (Giavarina 2015), constructing Bland–Altman plots and recording relevant values i.e. bias, standard deviation of the differences and limits of agreement. Again, this was done for the four considered hcPTT methodologies.

3. Results

Of the total number of datasets gathered at each of the two measurement sites (600), 94%, 93.6%, 94.4% and 94.4% yielded a hcPTT for Base PTT_1, Base PTT_2, Apex PTT_1 and Apex PTT_2 respectively. On a per-patient level, 96 of the 100 patients yielded a final hcPTT for Base measurements. For the Apex measurements, 97 patients yielded a final hcPTT. Sphygmocor cfPTT reference values were gathered from 97 of the 100 patients.

3.1. Correlation with clinical parameters and Sphygmocor cfPTT

Figure 3 shows the distributions of all four hcPTT estimates versus age, per patient. In case no error bar is visible, it is assumed that for two out of the three measurements no hcPTT estimate was possible (due to low signal quality or issues with the ECG). Panels (A) and (B) show the significant correlations, between age and Base PTT_1 ($\rho = -0.3, p = 0.003$) and PTT_2 ($\rho = -0.377, p < 0.001$) respectively. Panels (C) and (D) show the same correlations, but for the Apex measurement site ($\rho = -0.144, p = 0.16$ and $\rho = -0.149, p = 0.146$).

In figure 4 the correlations are depicted for Base PTT_1 and PTT_2, with Sphygmocor cfPTT. This figure highlights the strongest correlations found between LDV-based hcPTT and any other metric in the analysis.

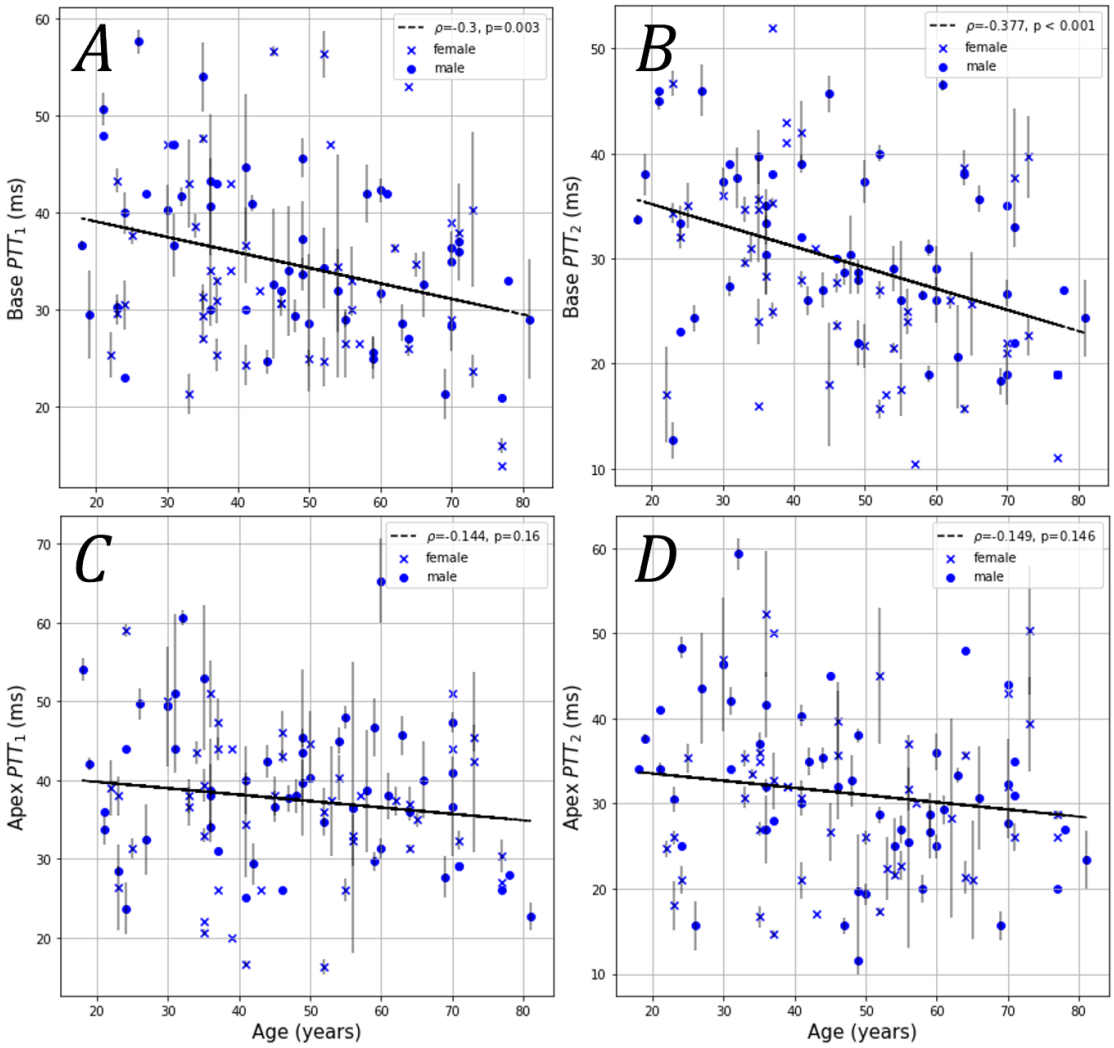

Figure 3. Correlations of the four proposed hcPTT estimations with age. Linear regression lines are drawn. The distinction between male and female patients has been visualized. Pearson-correlation coefficients and their p-values are given. Error bars represent the standard deviation of the resulting hcPTT values for the three measurements done per patient.

Base PTT_1 and Sphygmocor cfPTT yielded a correlation with $\rho = 0.359$ and $p < 0.001$, Base PTT_2 and Sphygmocor cfPTT yielded $\rho = 0.475$ and $p < 0.001$.

In table 2, the Pearson-correlation coefficients between the considered hcPTT values and other parameters such as brachial SBP and DBP, and Sphygmocor cfPTT are displayed.

3.2. Relation between hcPTT methods

Correlation between PTT_1 and PTT_2 for Base ($N = 96$) and Apex ($N = 97$) separately are investigated in figure 5. The distributions are accompanied by their respective Bland–Altman plots. The correlation between Base PTT_1 and Base PTT_2 yields the highest coefficient. the mean difference of these two is −5.08 ms. Both the paired t-test ($T - statistic = 5.545, p < 0.001$) and Wilcoxon signed ranks test ($Test - Statistic = 950, p < 0.001$) suggest a significant difference between these two methods. The mean difference between Apex PTT_1 and Apex PTT_2 is -6.32 ms. The paired t-test ($T - statistic = 5.315, p < 0.001$) and Wilcoxon signed ranks test ($Test - Statistic = 879, p < 0.001$) provide similar results as with the Base hcPTT methods. The limits of agreement are large for both measurement sites.

Figure 6 explores the correlations between measurement sites while controlling for the hcPTT estimation methods ($N = 96$). PTT_2 reports the highest correlation between Base and Apex. Bland–Altman figures for these cases show next to no bias (mean difference of 1.62 and 2.81 ms for PTT_2 and PTT_1 respectively), although a large variance is again observed. All correlations are given in table 3.

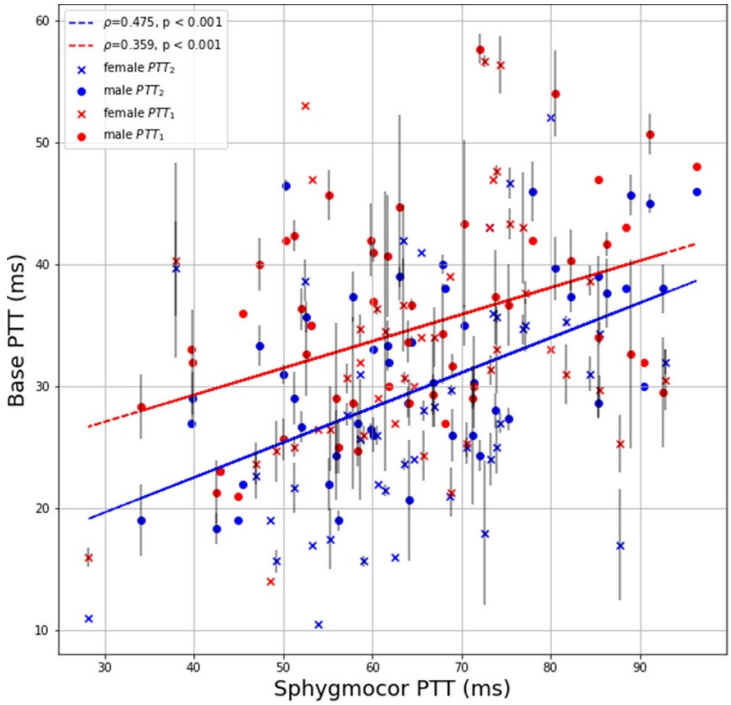

Figure 4. Correlations are depicted between both hcPTT estimation methods on Base measurements, and the golden standard of Sphygmocor cfPTT. Pearson correlations are given with their *p*-values for both cases. Linear regression lines are drawn in the relevant color.

Table 2. Pearson-correlation coefficients of the proposed hcPTT estimations with age, brachial SBP, and DBP, and cfPTT are shown. Highlighted with '*' are the statistically significant correlations with a *p*-value smaller than 0.05. ('**' and '***' refer to *p*-values smaller than 0.01 and 0.001 respectively).

	Base PTT_1	Base PTT_2	Apex PTT_1	Apex PTT_2
Age	-0.3^{**}	-0.377^{***}	−0.144	−0.149
SBP	-0.259^{*}	−0.18	−0.058	−0.1
DBP	−0.179	−0.098	−0.047	−0.125
cfPTT	0.359^{***}	0.475^{***}	0.167	0.196

3.3. Intra- and inter-operator variability

Not all data measured on the 10 subjects was fit for analysis. In one case, only two of the three measurements were conducted. Another two cases contained one measurement of inadequate signal quality each. This resulted in 111 out of the total 120 (92.5%) planned measurements that could be used.

The intra-operator variability is low (CV $< 15\%$) for both operators, for all four methodologies. Specifically OP2 has very low (CV $< 5\%$) variability. Especially the SE of OP2 for Base PTT_1 suggests minimal variability in the estimate of its mean CV. The other SEs range between 14.5% and 33% of their respective mean CV estimates. Mean CV and their SEs are given in table 4.

Figure 7 displays the Bland–Altman analysis done on the subject-level hcPTT estimates for OP1 and OP2. It was observed that both the bias and limits of agreement are smallest for Base PTT_2, suggesting that this hcPTT estimation method is the most reproducible between different operators. Notably, measurements taken at the Apex seem to produce results with higher biases, and wider limits of agreement, insinuating less reproducibility.

4. Discussion

Despite the compelling evidence of PWV as a biomarker of cardiovascular risk and target organ damage, its widespread application is still hampered by the difficulty of its measurement. LDV, picking up vibrations from the skin, has the potential to provide an easy technique to be broadly deployed, beyond specialized centers. Our team has been successful in using integrated silicon photonics solutions to develop a multi-sensor LDV system to simultaneously acquire signals from two distinct locations, and we previously demonstrated to be able to measure cfPWV.

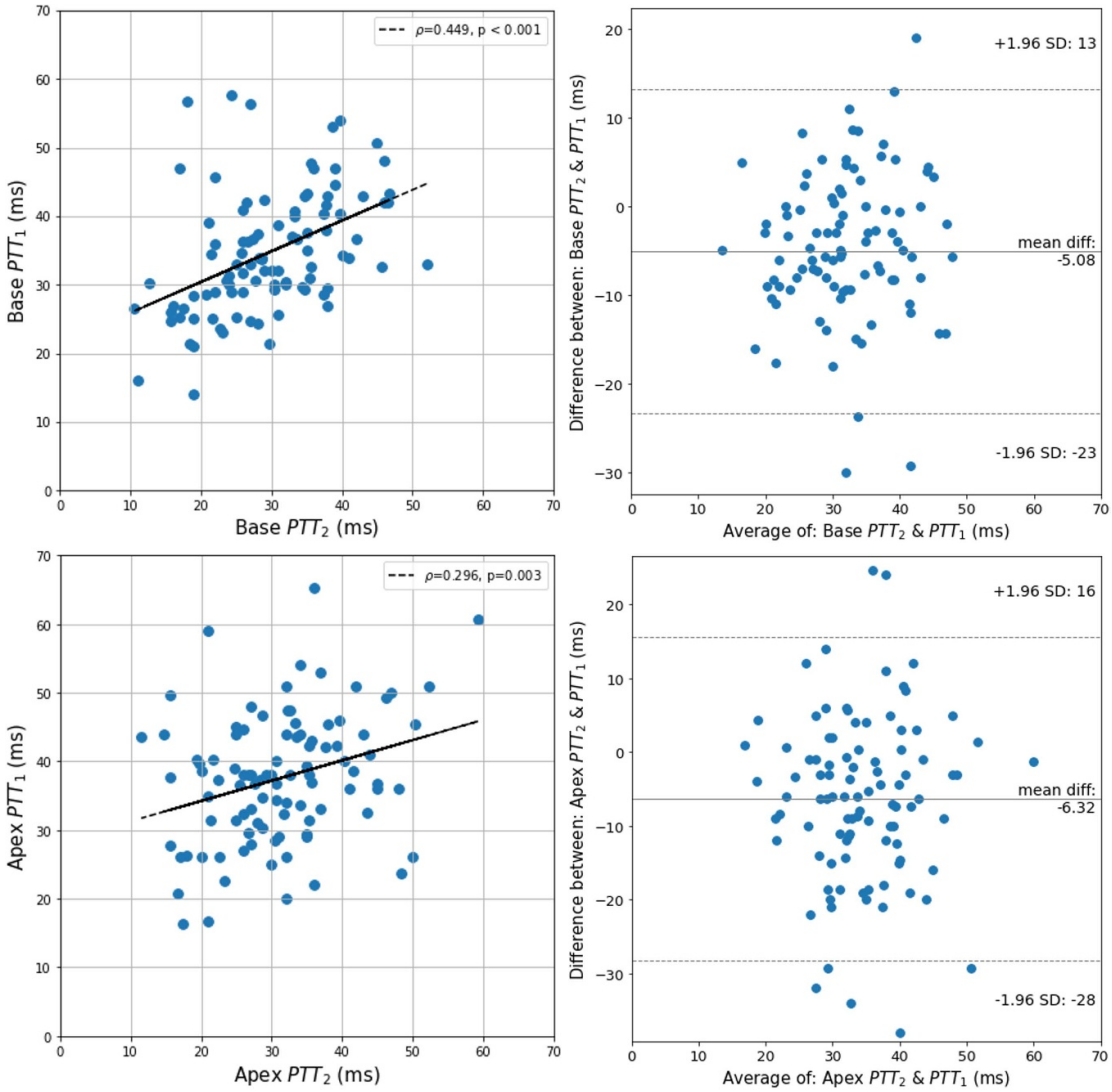

Figure 5. Correlations between the two proposed hcPTT-estimation methods are investigated while controlling for the heart-signal measurement site. Bland–Altman plots are displayed in addition. SD refers to the standard deviation of the differences between the two datasets.

4.1. Feasibility of LDV-based hcPTT

In this study, we explored the use of our LDV-based prototype to also measure heart-carotid PTTs and demonstrated that it is feasible to capture signals from two different locations on the chest that seemingly demonstrate a high similarity to seismocardiographic signals and hence potentially allow identifying moments of aortic valve opening and closure. Combined with simultaneous measurements at the carotid artery, we could measure PTTs at aortic valve opening (PTT_1) and closure (PTT_2). PTT_2 using the 'Base' location on the chest provided the strongest correlations with age and blood pressure, and was also the measurement with the lowest inter- and intra-operator variability.

Irrespective of the exact method (PTT_1, PTT_2, Base or Apex), hcPTT could be estimated in about 94% of the population, with a very good inter- and intra-operator variability. These numbers, however, should be interpreted within the context of the study. It is observed from figure 3 that several data-points show no error bars, which inherently means that of the three measurements for the considered heart-carotid measurement site, at least one did not yield a hcPTT estimate. Some measurements contained a faulty ECG trace (3.2% for Base and 2.8% for Apex measurements), but for the remainder 2.8% of measurements, this lack of a hcPTT could be attributed to a low signal quality or less interpretable waveforms for at least one of the measuring locations, with the carotid signals only failing for 5 measurements. The most difficult component in the estimation of hcPTT was the interpretation of the heart signals. Signal features associated with the first heartsound, on which PTT_1 was based, often fluctuated between patients in temporal and frequency content. The signal features corresponding with the second heartsound were not always as pronounced and sometimes difficult to detect. The ECG measurements in this feasibility study helped to identify signal

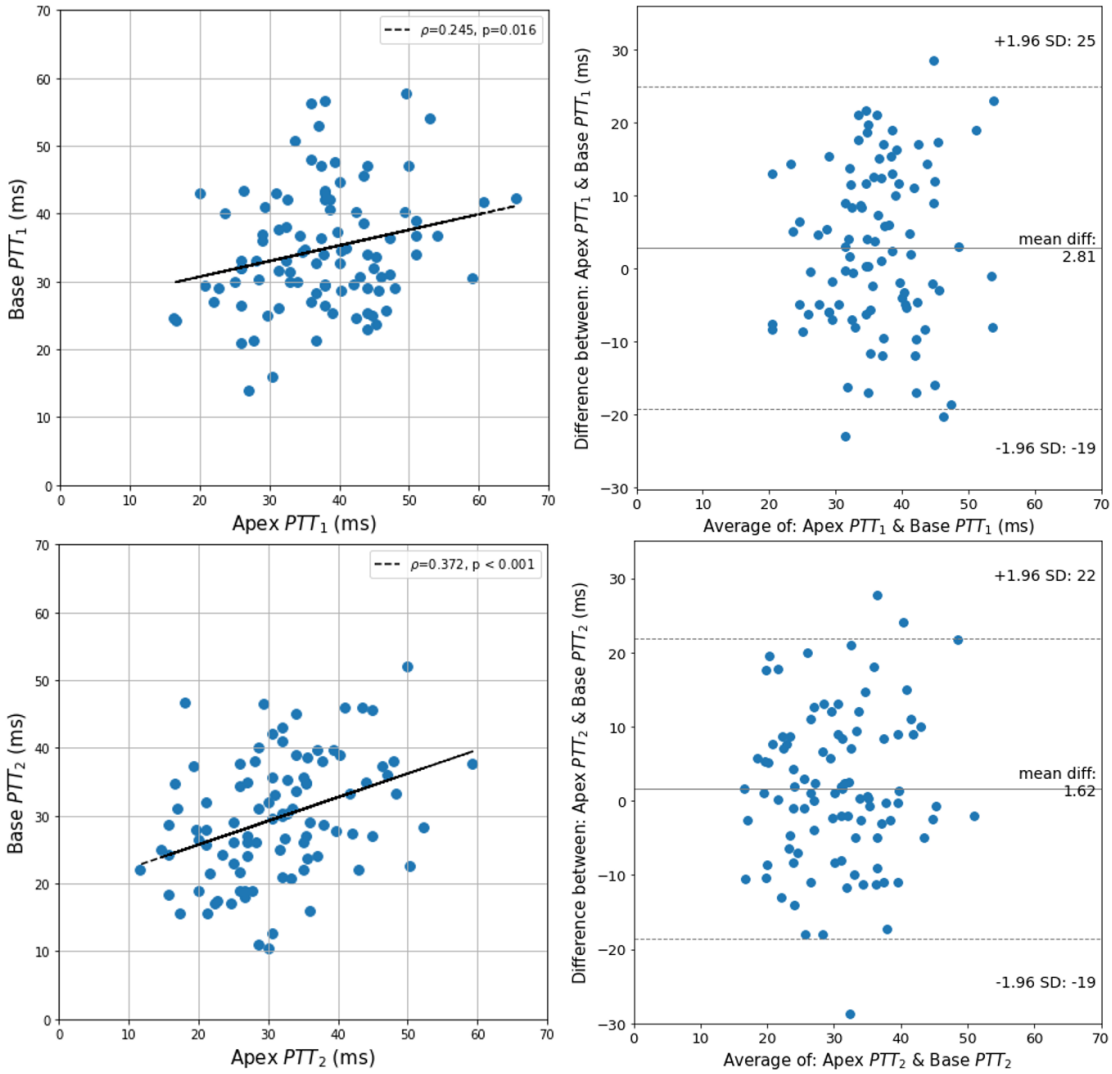

Figure 6. Correlations between the two heart-measurement sites are investigated while controlling for the hcPTT estimation method. Bland–Altman plots are displayed in addition.

features, but the method should become independent of the ECG. Any potential future work will implement algorithms for the automatic interpretation of the heart signals.

4.2. hcPTT as biomarker of arterial stiffness?

For hcPTT to be a biomarker of arterial stiffness, it should at least negatively correlate with its main predictor i.e. (chronological) age, as one may expect with an increased arterial stiffness. This is the case for hcPTT measured at the Base for both PTT_1 and PTT_2 (figure 3 and table 2), but not for values retrieved from apical data. We speculate that the consistent results for Base measurements are explained by the fact that the Base measurement site is anatomically closer to the aortic valve, leading to a better identifiability of the desired AO and AC features, with reduced distortion and delay of vibrations traveling to the measuring site. We found less pronounced correlations with brachial SBP, which was only significantly correlated with Base PTT_1, while brachial DBP did not significantly correlate with any of the measured hcPTT's.

These correlations are thus albeit modest, but it is important to consider that we are analyzing hcPTT, and not hcPWV which requires knowledge of the pathlength (see also further). As we expected, we found a positive correlation between cfPTT and hcPTT, with again the highest values for hcPTT assessed at the base ($\rho = 0.359$, $p < 0.001$ and $\rho = 0.475$, $p < 0.001$ for PTT_1 and PTT_2, respectively). Given that heart-carotid and carotid–femoral sample a very different trajectory along the arterial tree, it may not be surprising to find moderate correlations between both.

While we only assessed hcPTT in this study, the ambition is to assess stiffness, and to eventually retrieve hcPWV, for which the pathlength is required. Nagasaki *et al* calculate heart-carotid distance as a function of height (HT); $dx = 0.2473 \times \mathrm{HT} - 18.999$ (2011). When this function is applied to the Base PTT_2 data of this

Table 3. Correlations between the four proposed hcPTT estimation methods. Highlighted with '*' are the statistically significant correlations with a p-value smaller than 0.05 ('**' and '***' refer to p-values smaller than 0.01 and 0.001 respectively).

	Base PTT_1	Base PTT_2	Apex PTT_1	Apex PTT_2
Base PTT_1	1	0.449***	0.245*	0.213*
Base PTT_2	0.449***	1	0.092	0.372***
Apex PTT_1	0.245*	0.092	1	0.296**
Apex PTT_2	0.213*	0.372***	0.296**	1

Table 4. Mean CV's are reported per hcPTT-acquiring method, together with their standard errors. N indicates the number of included subjects in the analysis.

	Intra operator 1			Intra operator 2		
	Mean CV (%)	SE	N	Mean CV (%)	SE	N
Base PTT_1	5.43	1.11	9	4.15	0.51	10
Base PTT_2	5.49	1.98	10	8.04	3.18	10
Apex PTT_1	9.27	3.59	9	11.75	3.30	10
Apex PTT_2	5.83	2.51	9	8.22	3.84	9

study, the average hcPWV (±standard deviation) was 8.89 ± 3.21 m s^{-1}, with a range of 3.47–22.88 m s^{-1}. These values are plausible, but given the absence of a reference, it is difficult to evaluate the accuracy of these estimates. What we do know is that none of the hcPWV estimates provided stronger correlations with age or blood pressure than hcPTT. In this feasibility study, we wanted to exclude sources of uncertainty beyond the uncertainty related to the LDV measurements, which is why we opted to present the results in terms of hcPTT.

An interesting aspect of our technique is that we assess hcPTT at both diastolic (PTT_1) and end-systolic pressure (PTT_2). Given that elastic arteries typically stiffen with an increasing pressure (Hermeling 2012), leading to lower PTT, one expects higher values for PTT_1 than for PTT_2. The Bland–Altman plots in figure 5 demonstrate that this is effectively the case on average, with an average difference, for the Base measurements, of 5.08 ms. Using the estimated path lengths from Nagasaki *et al* this time difference translates into an average hcPWV difference of 1.53 ± 2.84 m s^{-1} (range: -4.24–13.82 m s^{-1}). This is lower than the ΔPWV $= 2.4$m s^{-1} (range: 0.8–4.4 m s^{-1}) stiffening reported by Hermeling *et al* for the carotid artery (2012).

However, an important consideration is that while we found this higher hcPTT at diastolic pressure on average, we did not find a systematic difference per subject (although the statistical tests performed did indicate a significant difference between PTT_1 and PTT_2). An important factor contributing to the observed variability is the complexity of the LDV signals originating from the aortic valve, but only being picked up at the skin-level. The effect of this on the time and frequency content of the observed epochs more than likely introduces inaccuracies in one or both PTT methods. Clearly PTT_1 is the most difficult to measure due to the complex waveform of S1 in the heart-LDV signals and the uncertainty on the identification of the exact timepoint of the opening of the aortic valve. While we are confident that further optimization of our technique (measurements directly on the skin without retroreflective patch and further signal processing enhancement) will further improve PTT_2 estimation, uncertainty on PTT_1 may remain too large to reliably quantify the stiffening between diastolic pressure and the DN.

4.3. LDV-based hcPTT compared to other techniques

The following paragraphs provide an overview of the studies that we could identify in literature on (or including) hcPWV, demonstrating the relative paucity of articles investigating hcPTT or hcPWV. Faita *et al* conducted a feasibility study with $N = 8$, where they also combine signal features that correspond to the closure of the aortic valve via SCG at proximal and distal locations (Faita *et al* 2009). Nagasaki *et al* also combine AC signal features but use a combination of ECG and PCG at proximal, and tonometry at distal locations (2011). Nagasaki *et al* found hcPWV value of 8.45 ± 0.17 m s^{-1}, which had a correlation coefficient of 0.686 with age ($N = 276$). They calculated the distance dx as mentioned earlier.

Li *et al* get to hcPTT via calculation of PAT using ECG and the foot of the systolic upstroke in the Doppler spectral envelope using US at the left carotid (2015). The pre-ejection period was calculated the same way but with the US probe pointed at the aortic valve. They then calculated hcPTT as the difference between PAT and pre-ejection period. They found hcPTT values of 22.65 ± 11.92 ms and 25.61 ± 10.18 ms for patients with a carotid intima-media thickness (CIMT) of over 0.8 mm and lower than 0.8 mm

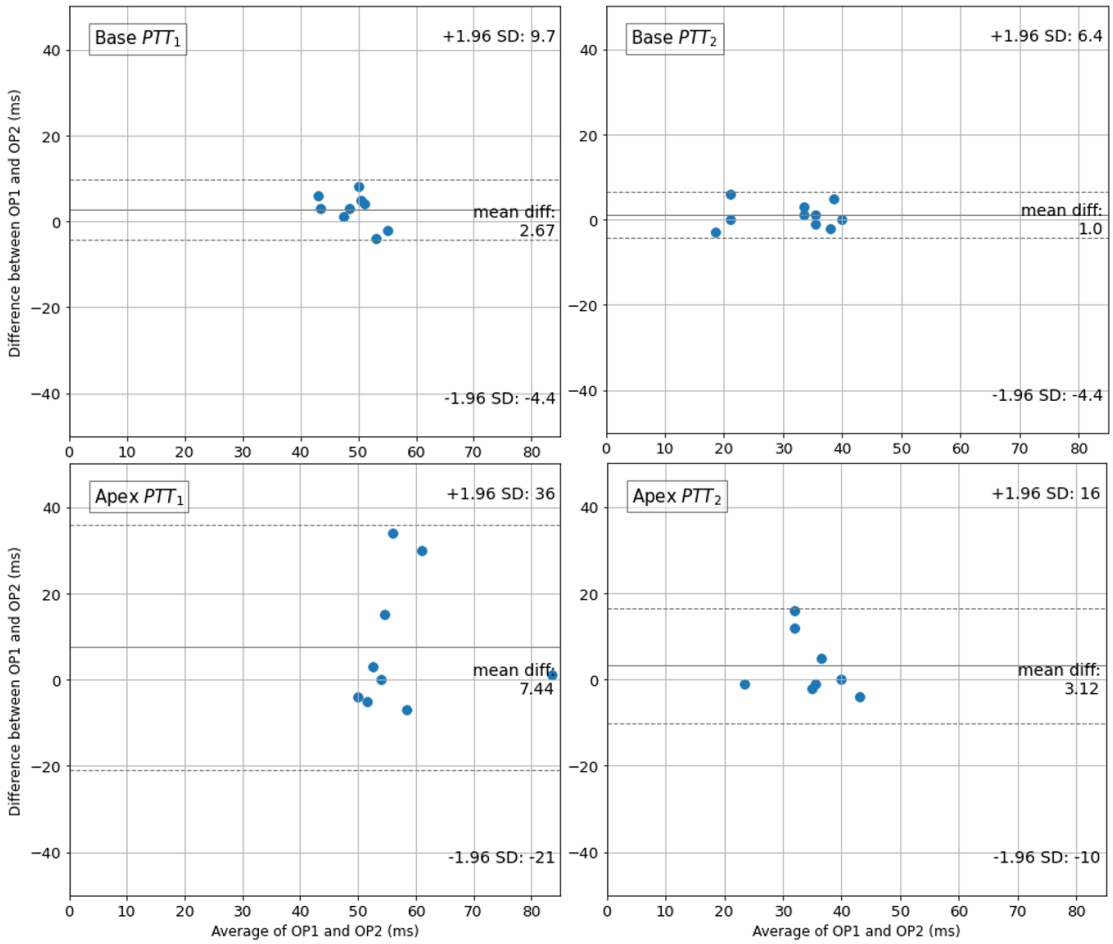

Figure 7. Bland–Altman plots are given for all four hcPTT methodologies. A comparison between hcPTT values, from measurements performed by two different operators, is made. SD refers to the standard deviation of the differences between the two datasets.

respectively ($N = 85$). The distance was calculated via the same way as Nagasaki *et al* This led to hcPWV values of 2.47 ± 0.49 ms and 2.35 ± 0.47 ms in the high and low CIMT group, respectively.

Yang *et al* calculate hcPTT as the time delay between the peak *R* wave in ECG, and the foot of the Doppler flow waveform with US (2019). They get to hcPWV by measuring *dx* with a tape measure on the body surface. This resulted in mean hcPWV values of 9.24 ± 1.93 m s^{-1} for their healthy controls, and 10.21 ± 4.18 m s^{-1} for patients with rheumatoid arthritis ($N = 127$). Ejiri *et al* found a median hcPWV value of 12.04 m s^{-1} with a standard deviation of 3.36 m s^{-1} in an elderly population (mean age of 79.2 ± 4.1 years, $N = 1351$) (2024).

When comparing between LDV and SCG, both methods require the application of an experimental tool to the skin. The used LDV prototype requires a piece of retroreflective tape, with SCG requiring the placement of accelerometers on the body. Currently, both technologies do not yet meet the expectations of clinicians and patients in that a vascular age assessment should come in the form of a quick, accessible and intuitive measurement. Future LDV technology developments aim for measurements without the need of the retroreflective patch (InSiDe project).

4.4. Study limitations

The eventual transition from hcPTT to hcPWV is only possible if hcPTT has been shown to indicate a change in arterial stiffness. A reliable distance metric *dx* has to be derived first, as to avoid adding errors to the hcPWV biomarker. Because of the shorter pathlength between both measurement sites, small distance errors will cause large relative hcPWV errors.

We did not investigate the technical reproducibility of this study. We strive towards hcPTT based on fully automated algorithms, removing the need of manual hcPTT estimation.

The most important limitation, however, is the absence of a proven reference method for LDV-derived hcPTT. The literature survey shows that no single method of estimating hcPTT (or hcPWV) is acceptable for

this role. A future study could consider using established methods that capture flow- or distensibility data at the aortic valve and carotid simultaneously, with a high enough temporal resolution, in order to acquire reference hcPTT data.

5. Conclusions

This work represents a feasibility study, investigating hcPTT as a potential and not well-known biomarker for arterial stiffening, sampling the properties of the large, proximal aorta and carotid artery using LDV technology to detect the PTT from the heart to the carotid artery. It was found that most robust hcPTT is retrieved from the base of the heart, and measurements are repeatable, with significant though moderate correlations with known predictors of arterial stiffness. Future work should focus on further refinement of the method—especially regarding the identification of aortic valve opening and closure from chest measurements—and on more precise validation against metrics of proximal aortic stiffness. We believe this work adds to the legitimacy of hcPWV as a biomarker that could be used in conjunction with cfPWV in the future.

Data availability statement

The data cannot be made publicly available upon publication because no suitable repository exists for hosting data in this field of study. The data that support the findings of this study are available upon reasonable request from the authors.

Acknowledgment

All work done in this article, was performed within the scope of the H2020-project: InSiDe (Grant agreement ID: 871547). The author's have confirmed that any identifiable participants in this study have given their consent for publication.

Ethical statement

The InSide study was approved by the National Ethics Committee and the French National Drug Agency (ANSM) on 28 November 2022, Clinicaltrial.gov number: NCT05711693.

Appendix

A.1. Sphygmocor cfPTT agreement with clinical parameters

Figure 8 shows the trends between Sphygmocor cfPTT and age ($\rho = -0.674, p < 0.001$), brachial SBP ($\rho = -0.512$, $p < 0.001$) and DBP ($\rho = -0.336$, $p = 0.001$). All correlations are statistically significant, with $N = 100$.

Figure 8 serves as a possible form of reference for hcPTT, with correlation values between cfPTT and age, SBP and DBP. We assume this because we consider cfPTT (and by extension: cfPWV), resulting from Sphygmocor measurements, as a golden standard for assessing vascular aging.

Currently it is not yet possible to approach the high correlation coefficient of $\rho = -0.674$ between Sphygmocor cfPTT and age when calculating hcPTT. At this time, we ascribe this effect to the different arterial pathway between both PTT's and increased complexity of the heart-LDV data. The proposed hcPTT's are clearly not yet interchangeable with Sphygmocor cfPTT, but could be considered as an additional metric that describes arterial stiffness in the ascending aorta, which is not included in the cfPWV pathway.

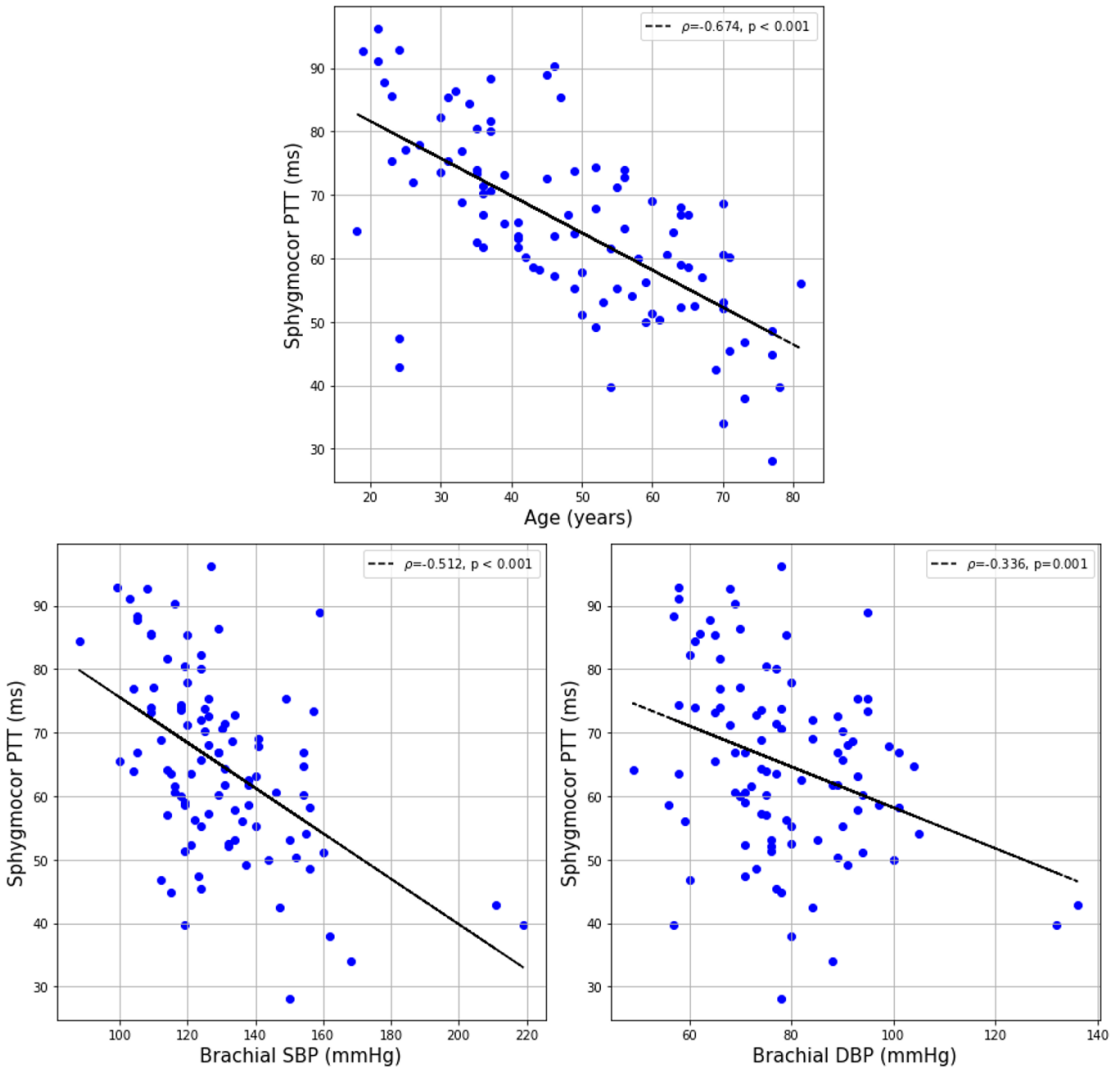

Figure 8. figure depicting reference correlations of Sphygmocor cfPTT with age, brachial SBP and DBP. Linear regression lines are drawn and correlation coefficients are given alongside their *p*-values.

ORCID iDs

Simeon Beeckman https://orcid.org/0009-0004-4590-9610
Smriti Badhwar https://orcid.org/0000-0002-6195-5316
Hakim Khettab https://orcid.org/0000-0001-8351-3845

References

Alastruey J *et al* 2023 Arterial pulse wave modeling and analysis for vascular-age studies: a review from VascAgeNet *Am. J. Physiol. Heart. Circ. Physiol.* **325** H1–H29

Badhwar S *et al* 2024 Clinical validation of carotid-femoral pulse wave velocity measurement using a multi-beam laser vibrometer: the CARDIS study *Hypertension* **81** 1986–95

Balali P, Rabineau J, Hossein A, Tordeur C, Debeir O and van de Borne P 2022 Investigating cardiorespiratory interaction using ballistocardiography and seismocardiography-a narrative review *Sensors* **22** 9565

Ben-Shlomo Y *et al* 2014 Aortic pulse wave velocity improves cardiovascular event prediction *J. Am. Coll. Cardiol.* **63** 636–46

Bensalah M Z, Bollache E, Kachenoura N, Giron A, De Cesare A, Macron L, Lefort M, Redheuil A and Mousseaux E 2014 Geometry is a major determinant of flow reversal in proximal aorta *Am. J. Physiol. Heart Circ. Physiol.* **306** H1408–16

Boutouyrie P and Bruno R-M 2019 The clinical significance and application of vascular stiffness measurements *Am. J. Hypertens.* **32** 4–11

Brandts A, van Elderen S G C, Tamsma J T, Smit J W A, Kroft L J M, Lamb H J, van der Meer R W, Westenberg J J M and de Roos A 2012 The effect of hypertension on aortic pulse wave velocity in type-1 diabetes mellitus patients: assessment with MRI *Int. J. Cardiovasc. Imaging* **28** 543–50

Campo A and Dirckx J 2011 Dual-beam laser Doppler vibrometer for measurement of pulse wave velocity in elastic vessels *22nd Congress Intl. Commission for Optics: Light for the Development of the World. Int. Society for Optics and Photonics* vol 8011 p 80118Y

Chirinos J A, Segers P, Hughes T and Townsend R 2019 Large-artery stiffness in health and disease: JACC state-of-the-art review *J. Am. Coll. Cardiol.* **74** 1237–63

Crow R S, Hannan P, Jacobs D, Hedquist L and Salerno D M 2017 Relationship between Seismocardiogram and Echocardiogram for Events in the Cardiac Cycle *Am. J. Noninvasive Cardiol.* **8** 39–46
De Melis M, Morbiducci U, Scalise L, Tomasini E P, Delbeke D, Baets R, Van Bortel L M and Segers P 2008 A noncontact approach for the evaluation of large artery stiffness: a preliminary study *Am. J. Hypertens.* **21** 1280–3
Di Lascio N, Bruno R M, Stea F, Bianchini E, Gemignani V, Ghiadoni L and Faita F 2014 Non-invasive assessment of carotid PWV via accelerometric sensors: validation of a new device and comparison with established techniques *Eur. J. Appl. Physiol.* **114** 1503–12
Dogui A, Kachenoura N, Frouin F'erique, Lefort M, De Cesare A, Mousseaux E and Herment A 2011 Consistency of aortic distensibility and pulse wave velocity estimates with respect to the Bramwell-Hill theoretical model: a cardiovascular magnetic resonance study *J. Cardiovasc. Magn. Reson.* **13** 11
Ejiri K *et al* 2024 Association of segment-specific pulse wave velocity with vascular calcification: the ARIC (atherosclerosis risk in communities) study *J. Am. Heart Assoc.* **13** e031778
Faita F, Gemignani V, Bianchini E, Bruno R M, Bombardini T and Ghiadoni L 2009 P9.04 a new method for continuous monitoring of central arterial stiffness during stress *Artery Res.* **3** 167
Giavarina D 2015 Understanding Bland Altman analysis *Biochem. Med.* **25** 141–51
Hermeling E *et al* 2012 The change in arterial stiffness over the cardiac cycle rather than diastolic stiffness is independently associated with left ventricular mass index in healthy middle-aged individuals *J. Hypertens.* **30** 396–402
Kaplan A D, O'Sullivan J A, Sirevaag E J, Lai P-H and Rohrbaugh J W 2012 Hidden state models for noncontact measurements of the carotid pulse using a laser Doppler vibrometer *IEEE Trans. Biomed. Eng.* **59** 744–53
Kim W Y *et al* 2007 Subclinical coronary and aortic atherosclerosis detected by magnetic resonance imaging in type 1 diabetes with and without diabetic nephropathy *Circulation* **115** 228–35
Laurent S, Cockcroft J, Van Bortel L, Boutouyrie P, Giannattasio C, Hayoz D, Pannier B, Vlachopoulos C, Wilkinson I and Struijker-Boudier H 2006 Expert consensus document on arterial stiffness: methodological issues and clinical applications *Eur. Heart J.* **27** 2588–605
Li C, Xiong H, Pirbhulal S, Wu D, Li Z, Huang W, Zhang H and Wu W 2015 Heart-carotid pulse wave velocity a useful index of atherosclerosis in Chinese hypertensive patients *Medicine* **94** e2343
Li Y *et al* 2020 Silicon photonics-based laser Doppler vibrometer array for carotid-femoral pulse wave velocity (PWV) measurement *Biomed. Opt. Express* **11** 3913–26
Li Y, Segers P, Dirckx J and Baets R 2013 On-chip laser Doppler vibrometer for arterial pulse wave velocity measurement *Biomed. Opt. Express* **4** 1229–35
Mancini V, Bergersen A W, Valen-Sendstad K and Segers P 2020 Computed poststenotic flow instabilities correlate phenotypically with vibrations measured using laser Doppler vibrometry : perspectives for a promising *in vivo* device for early detection of moderate and severe carotid stenosis *J. Biomech. Eng. Trans. ASME* **142** 13
Mancini V, Tommasin D, Li Y, Reeves J, Baets R, Greenwald S, Segers P and on behalf of the CARDIS consortium 2019 Detecting carotid stenosis from skin vibrations using Laser Doppler Vibrometry–an *in vitro* proof-of-concept *PLoS One* **14** e0218317
Mitchell G F, Hwang S-J, Vasan R S, Larson M G, Pencina M J, Hamburg N M, Vita J A, Levy D and Benjamin E J 2010 Arterial stiffness and cardiovascular events: the framingham heart study *Circulation* **121** 505–11
Mukkamala R, Hahn J-O, Inan O T, Mestha L K, Kim C-S, Töreyin H and Kyal S 2015 Toward ubiquitous blood pressure monitoring via pulse transit time: theory and practice *IEEE Trans. Biomed. Eng.* **62** 1879–901
Nagasaki T, Yamada S, Wakita Y, Imanishi Y, Nagata Y, Okamoto K, Yoda K, Emoto M, Ishimura E and Inaba M 2011 Clinical utility of heart-carotid pulse wave velocity in healthy Japanese subjects *Biomed. Aging Pathol.* **1** 107–11
Ou P, Celermajer D S, Jolivet O, Buyens F, Herment A, Sidi D, Bonnet D and Mousseaux E 2008a Increased central aortic stiffness and left ventricular mass in normotensive young subjects after successful coarctation repair *Am. Heart J.* **155** 187–93
Ou P, Celermajer D S, Raisky O, Jolivet O, Buyens F, Herment A, Sidi D, Bonnet D and Mousseaux E 2008b Angular (gothic) aortic arch leads to enhanced systolic wave reflection, central aortic stiffness and increased left ventricular mass late after aortic coarctation repair: evaluation with magnetic resonance flow mapping *J. Thorac. Cardiovasc. Surg.* **135** 62–68
Park H, Wei Q, Lee S and Lee M 2022 Novel design of a multimodal technology-based smart stethoscope for personal cardiovascular health monitoring *Sensors* **22** 6465
Parker K H 2009 A brief history of arterial wave mechanics *Med. Biol. Eng. Comput.* **47** 111–8
Pereira T, Correia C and Cardoso J 2015 Novel methods for pulse wave velocity measurement *J. Med. Biol. Eng.* **35** 555–65
Redheuil A, Yu W-C, Wu C O, Mousseaux E, de Cesare A, Yan R, Kachenoura N, Bluemke D and Lima J A C 2010 Reduced ascending aortic strain and distensibility: earliest manifestations of vascular aging in humans *Hypertension* **55** 319–26
Segers P, Rietzschel E R and Chirinos J A 2020 How to measure arterial stiffness in humans *Arteriosclerosis, Thrombosis Vascular Biol.* **40** 1034–43
Seoni S, Beeckman S, Li Y, Aasmul S, Morbiducci U, Baets R, Boutouyrie P, Molinari F, Madhu N and Segers P 2022 Template matching and matrix profile for signal quality assessment of carotid and femoral laser Doppler vibrometer signals *Front. Physiol.* **12** 775052
van Elderen S G C, Brandts A, Westenberg J J M, van der Grond J, Tamsma J T, van Buchem M A, Romijn J A, Kroft L J M, Smit J W A and de Roos A 2010 Aortic stiffness is associated with cardiac function and cerebral small vessel disease in patients with type 1 diabetes mellitus: assessment by magnetic resonance imaging *Eur. Radiol.* **20** 1132–8
Vlachopoulos C, Aznaouridis K and Stefanadis C 2010 Prediction of cardiovascular events and all-cause mortality with arterial stiffness: a systematic review and meta-analysis *J. Am. College Cardiol.* **55** 1318–27
Westerhof N, Lankhaar J-W and Westerhof B E 2009 The arterial windkessel *Med. Biol. Eng. Comput.* **47** 131–41
Wolinsky H and Glagov S 1967 A lamellar unit of aortic medial structure and function in mammals *Circ. Res.* **20** 99–111
Yang C and Tavassolian N 2018 Pulse transit time measurement using seismocardiogram, photoplethysmogram and acoustic recordings: evaluation and comparison *IEEE J. Biomed. Health Inf.* **22** 733–40
Yang Y, Wang Z, Fu Z, Yang R, Wang J, Yuan L, Gao F and Duan Y 2019 Stiffening of aorta is more preferentially associated with rheumatoid arthritis than peripheral arteries *Rheumatol. Int.* **39** 1711–21